CHLAMYDOMONAS FLAGELLAR MUTANTS LACKING RADIAL SPOKES AND CENTRAL TUBULES

Structure, Composition, and Function of Specific Axonemal Components

G. B. WITMAN, J. PLUMMER, and G. SANDER

From the Department of Biology, Princeton University, Princeton, New Jersey 08540

ABSTRACT

The fine structure, protein composition, and roles in flagellar movement of specific axonemal components were studied in wild-type *Chlamydomonas* and paralyzed mutants *pf-14*, *pf-15A*, and *pf-19*. Electron microscope examination of the isolated axoneme of *pf-14* showed that it lacks the radial spokes but is otherwise structurally normal. Comparison of isolated axonemes of wild type and *pf-14* by sodium dodecyl sulfate-acrylamide gel electrophoresis indicated that the mutant is missing a protein of 118,000 mol wt; this protein is apparently a major component of the spokes. *Pf-15A* and *pf-19* lack the central tubules and sheath; axonemes of these mutants are missing three high molecular weight proteins which are probably components of the central tubule-central sheath complex. Under conditions where wild-type axonemes reactivated, axonemes of the three mutants remained intact but did not form bends. However, mutant and wild-type axonemes underwent identical adenosine triphosphate-induced disintegration after treatment with trypsin; the dynein arms of the mutants are therefore capable of generating interdoublet shearing forces. These findings indicated that both the radial spokes and the central tubule-central sheath complex are essential for conversion of interdoublet sliding into axonemal bending. Moreover, because axonemes of *pf-14* remained intact under reactivating conditions, the nexin links alone are sufficient to limit the amount of interdoublet sliding that occurs.

The axial periodicities of the central sheath, dynein arms, radial spokes, and nexin links of *Chlamydomonas* were determined by electron microscopy using the lattice-spacing of crystalline catalase as an internal standard. Some new ultrastructural details of the components are described.

KEY WORDS cilia · flagella · axonemes · *Chlamydomonas* · mutants · motility

According to the sliding microtubule model (6, 30, 31), the basis for ciliary and flagellar movement is an adenosine triphosphate (ATP)-induced interaction of the arms of the outer doublets with the B-tubules of the adjacent outer doublets, resulting in active sliding between doublet microtubules. When this sliding is resisted by structures within the axoneme, axonemal bending results. Evidence supporting this model includes demonstrations that outer doublets slide relative to one another during ciliary bending (30), that interdoublet sliding is induced by ATP (33), and that the arms of the outer doublets contain ATPase

activity (14) and are directly involved in interdoublet sliding (15). Less evidence is available concerning how interdoublet sliding is converted into bending, and what specific axonemal structures are involved in this process. Summers and Gibbons (33, 34) observed that when isolated axonemes of sea urchin sperm flagella were treated with trypsin, the radial spokes and nexin links were specifically disrupted. When ATP was added to the trypsin-treated axonemes, the outer doublets literally slid apart, indicating that the spokes and links were normally responsible for limiting the amount of interdoublet sliding and for converting this sliding into axonemal bending. Warner and Satir (37) provided ultrastructural evidence that the radial spokes and the central sheath interact during bend formation in mussel gill cilia; they concluded that these interactions were part of the mechanism for converting microtubule sliding into bending. However, there is no direct evidence for the roles of any specific axonemal components in the control of sliding and in the actual formation of the flagellar bend.

To learn more about the components involved in these processes, we have been studying mutants of *Chlamydomonas* having a defective flagellar apparatus. A number of mutants are available in which the cells are paralyzed or move their flagella abnormally (19, 24, 38); some of these mutants are missing specific axonemal structures (38, 42). By correlating the presence or absence of these structures with the ability of the axoneme to undergo particular parts of the movement generating process, e.g. interdoublet sliding or axonemal bending, the roles of the individual structures in flagellar movement can be determined. Similarly, by comparing proteins of axonemes of these mutants with those of wild type, the proteins contained in the missing or defective components can be identified.

In this report we compare the fine structure, protein composition, reactivation, and ATP-induced disintegration of axonemes of wild-type *Chlamydomonas* and three mutants: one missing the radial spokes (42), and two missing the central tubules and central sheath (38). The results confirm and extend our knowledge of flagellar fine structure, indicate some of the proteins contained in these structures, and provide direct evidence that the radial spokes and central sheath are involved in flagellar bend formation. The results also indicate that the nexin links limit the amount of sliding between adjacent outer doublets.

MATERIALS AND METHODS

Strains and Growth Conditions

The *Chlamydomonas reinhardii* wild-type strain, *1132D(−)*, and three paralyzed mutants, *pf-14(−)*, *pf-15A(+)*, and *pf-19(+)*, were obtained from Dr. Gary Borisy, Dept. of Molecular Biology and Biophysics, University of Wisconsin, Madison, Wis. Cells were grown in 2-liter Erlenmeyer flasks containing 1.5 liters of Sager and Granick's Medium I (29), modified by addition of three times the normal amount of potassium phosphate. Cultures were bubbled with air containing 5% CO_2, and stirred with magnetic stirrers. Cell growth was synchronized on a cycle of 14 h light and 10 h dark. Cultures were usually used in the 6th h of the light cycle, at a density of about 1×10^6 cells/ml.

Isolation of Axonemes

In earlier experiments, flagella were detached and demembranated by treating whole cells with 0.05% Nonidet P-40 (Shell Chemical Co., New York), and the axonemes were isolated, as described by Allen and Borisy (2). However, this procedure frequently resulted in contamination of the axonemal pellet by cellular debris, particularly in the large-scale preparations needed for biochemical studies. In more recent experiments, we have obtained axonemes from flagella isolated by a modification of the dibucaine procedure developed by Thompson et al. (35) for deciliation of *Tetrahymena*.[1] Cells were harvested by centrifugation at 600 *g* (1,500 rpm, IEC 253 or 259 swinging bucket head) for 5 min, washed twice in 10 mM *N*-2-hydroxyethylpiperazine-*N'*-2-ethane sulfonic acid (HEPES) (pH 7.4), and resuspended in 10 ml of HMDS (10 mM HEPES, pH 7.4; 5 mM $MgSO_4$; 1 mM dithiothreitol [DTT]; 4% sucrose) at room temperature. The cell suspension was then pipetted into a 50-ml conical centrifuge tube containing 2 ml of 25 mM dibucaine HCl[2] (Nupercaine HCl, CIBA Pharmaceutical Co., CIBA-GEIGY Corp., Summit, N. J.). The suspension was then drawn gently in and out of a 10-ml Falcon disposable plastic pipette several times. After 2–5 min, nearly all cells were deflagellated, and the suspension was diluted with 20 ml of ice-cold HMDS containing 0.25 mM ethylene glycol-bis(β-aminoethyl ether)*N,N,N',N'*-tetraacetate (EGTA). Cell bodies were removed by centrifugation at 4°C for 7 min at 1,550 *g* (IEC 253 head, 2,400 rpm). The supernate was collected and recentrifuged as above. The cell-free su-

[1] We wish to thank Drs. Keith Summers and Martin Flavin for showing us that this procedure was applicable to *Chlamydomonas*, and we are grateful to Rose Fay for her valuable assistance in developing conditions permitting reactivation of flagella isolated by this procedure.

[2] 2-butoxy-*N*-(2-diethylaminoethyl) cinchoninamide hydrochloride.

pernate was then centrifuged at 4°C at 31,000 *g* (Sorvall SS-34 rotor, 16,000 rpm [DuPont Instruments-Sorvall, DuPont Co., Wilmington, Del.]) for 20 min. The resulting pellet contained whole, intact flagella and was virtually free of contamination by cells and nonflagellar cell components. The flagella were then demembranated by resuspension in 5 ml of ice-cold 0.04–1% Nonidet in HMDEKP (30 mM HEPES, pH 7.4; 5 mM $MgSO_4$; 1 mM DTT; 0.5 mM Na_2 EDTA; 25 mM KCl; 0.5% polyethylene glycol, 20,000 mol wt). The demembranated axonemes were collected by centrifugation at 4°C at 31,000 *g* for 20 min, gently resuspended in 5 ml of cold HMDEKP, recentrifuged as above, and finally resuspended in 1 ml of fresh cold HMDEKP. Axonemes obtained by this procedure were virtually free of cellular contamination, and up to 100% of the axonemes could be reactivated. This procedure also permits recovery of the flagellar membrane and matrix components.

Protein concentrations were determined by the method of Lowry et al. (20).

Reactivation of Axonemes

Axonemal reactivation was carried out essentially as described by Allen and Borisy (2). A small aliquot of axonemes in HMDEKP was mixed on a microscope slide with an equal volume of 2 mM ATP in HMDEKP, and observed by means of dark-field optics in a Zeiss Universal Microscope (Carl Zeiss, Inc., N. Y.) fitted with an Ultracondenser and a 40x Planappochromat objective. For reactivation, it was essential to use microscope slides that had been thoroughly cleaned with detergent and rinsed with distilled water; axonemes would not reactivate on "precleaned" slides direct from the manufacturer's package. Axonemes also had a tendency to stick down to the surface of the glass slide and cover slip; this problem could be partially alleviated by using quartz slides and cover slips, or by coating glass slides and cover slips with Siliclad (Becton, Dickinson & Co., Rutherford, N. J.). However, the best reactivation was obtained with clean glass slides and cover slips that had been coated with a thin layer of carbon in a vacuum evaporator.

ATP-Induced Disintegration of Trypsin-Treated Axonemes

Sliding of outer doublets was induced by mixing isolated axonemes in HMDEKP with trypsin (at a trypsin to axonemal protein ratio of 1:600 to 1:1,500) and ATP (0.1 to 1.0 mM final concentration). Axonemal disintegration was observed by dark-field light microscopy as above, or was monitored by measuring the decrease in turbidity (absorbance) at 350 nm in a Gilford 250 spectrophotometer (Gilford Instrument Laboratories, Oberlin, Ohio) equipped with an automatic cuvette programmer and a recorder (34).

Light Microscope Photography

Dark-field micrographs were taken on Kodak 2475 Recording Film and processed at ASA 4000. For stroboscopic illumination, a Chadwick-Helmuth Strobe Model 136 power supply and Model 762 lamp (Chadwick-Helmuth Co., Inc., Monrovia, Calif.) were triggered by a General Radio Model 1310-A audio oscillator.

Electron Microscopy

THIN SECTIONS: Isolated axonemes in HMDEKP at 0°C were mixed with an equal volume of cold 4% glutaraldehyde in 50 mM sodium cacodylate, pH 7.4. After 30-min fixation, the axonemes were pelleted by centrifugation at 17,000 *g* (Sorvall SS-34 rotor, 12,000 rpm [DuPont Instruments-Sorvall]) for 30 min. The pellet was postfixed for 30 min in 1% OsO_4 in 50 mM cacodylate buffer, pH 7.4, which was added cold and allowed to come to room temperature during the fixation. The pellets were then dehydrated and embedded in Epon (21). Light grey-to-gold thin sections were cut on an LKB Ultratome III (LKB Instruments, Inc., Rockville, Md.), mounted on uncoated 400-mesh or carbon-over-Formvar-coated 200-mesh grids, and stained with 5% aqueous uranyl acetate for 20 min followed by Reynolds' lead citrate for 5 min (27).

NEGATIVE STAINS: A drop of the axonemal suspension was placed on a carbon-over-formvar-coated 200-mesh grid. After a few seconds, most of the drop was drained away. The grid was then rinsed with a few drops of aqueous 1% uranyl acetate. Excess uranyl acetate was drawn off with filter paper, leaving a thin film of stain which was then air-dried.

MAGNIFICATION CALIBRATION: Spacings of axonemal structures were determined using crystalline catalase as an internal standard (22, 43). Catalase crystals were fixed in glutaraldehyde (43) and mixed with axonemes before negative staining with uranyl acetate. Micrographs were taken which contained both catalase crystals and disrupted axonemes in the same field (Fig. 2*a*); the catalase crystal lattice spacing and the axonemal spacings were then measured directly from the films with a Nikon Model 6 comparator (Nikon Inc., Garden City, N. Y.) with a 10× lens. The value of 87.5 Å reported by Wrigley (43) for the lattice spacing was used in determining the magnification factor. A check of the lattice spacing using a carbon replica of an optical diffraction grating gave a value of 87.3 ± 1.1 Å, in good agreement with Wrigley's figure.

Acrylamide Gel Electrophoresis

SDS-acrylamide gel electrophoresis of axonemal proteins was carried out in slab gels by the procedures of Laemmli (17) and Laemmli and Favre (18). Axonemal pellets were resuspended in "final sample buffer" (3% SDS, 10% glycerol, 0.001% bromphenol blue, 0.0625

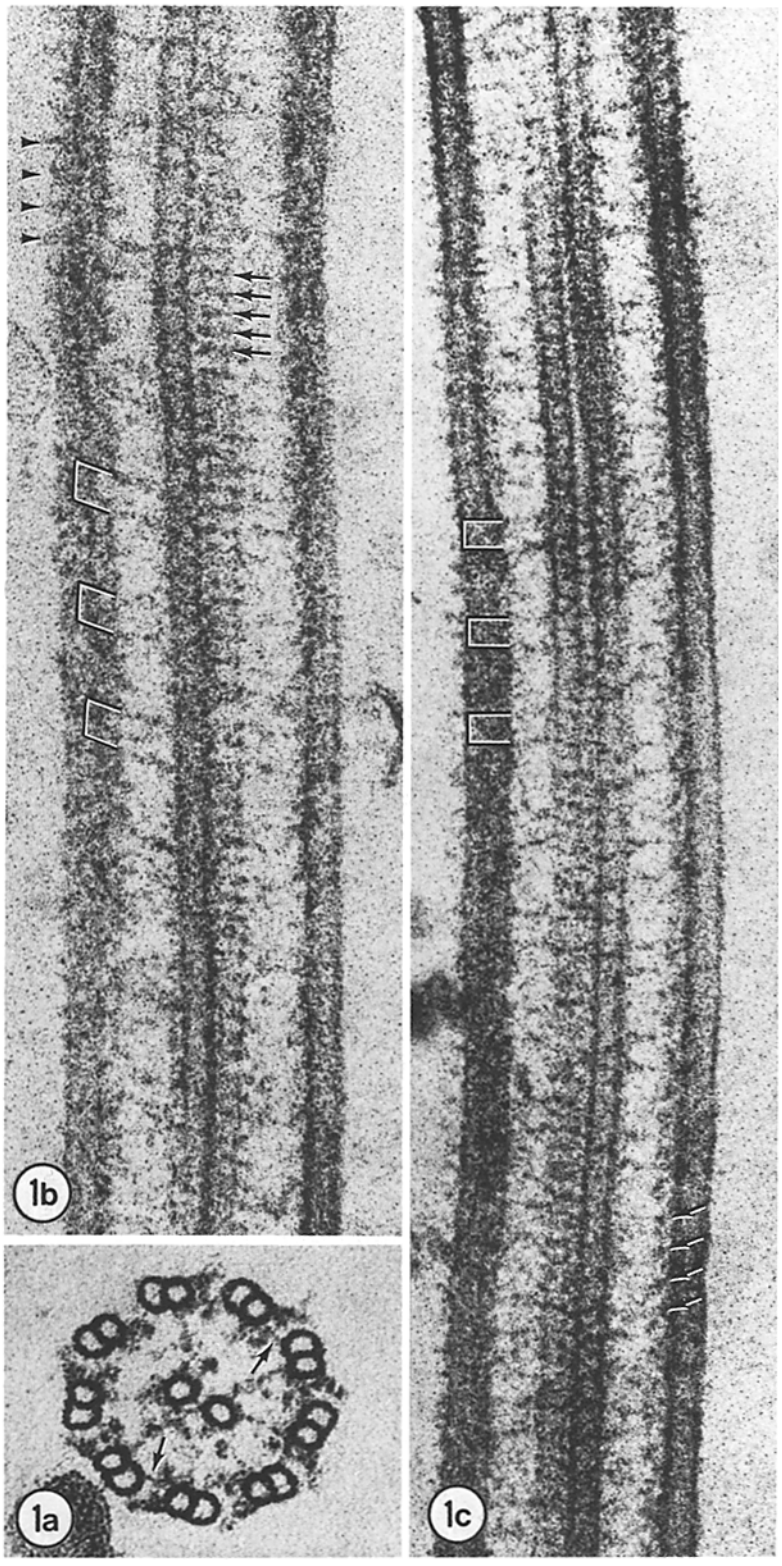
1b
1a
1c

M Tris-HCl, pH 6.8), heated for 2 min at 100°C, and frozen until used. Immediately before electrophoresis, samples were made 5% in 2-mercaptoethanol and heated again for 2 min at 100°C. Separating gels contained 7% acrylamide; stacking gels contained 3% acrylamide. The running buffer contained 1 g of SDS, 3 g of Tris, and 14.4 g of glycine in 1,000 ml of water. Gels were fixed and stained in 50% trichloroacetic acid containing 0.1% Coomassie brilliant blue, and destained in 7% acetic acid.

Molecular weights of axonemal proteins were estimated by comparing their relative electrophoretic mobilities to those of proteins of known molecular weight. Proteins used as molecular weight standards were: glyceraldehyde-3-phosphate dehydrogenase (36,000), ovalbumin (43,000), porcine brain tubulin (55,000), bovine serum albumin (68,000), phosphorylase a (94,000), β-galactosidase (130,000), and myosin (220,000).

RESULTS

Ultrastructural Observations

WILD TYPE: Many details of the fine structure of the *Chlamydomonas* axoneme have been described previously (2, 10, 16, 28, 41); these axonemes have the same basic design as those of other "9+2" flagella. The wild-type (*1132D*) axoneme contains two central microtubules and nine outer doublet microtubules; each outer doublet microtubule is itself made up of an A-tubule and a B-tubule (Fig. 1*a*). Attached to the A-tubule are the inner and outer dynein arms, which extend toward the B-tubule of the adjacent doublet. These arms repeat along the outer doublet (Figs. 1*b*, *c*, and 2*a*); measurement of their period in negatively stained material, using the lattice spacing of crystalline catalase as an internal standard of length, indicated that they have an axial spacing of 250 Å (see Table I).

Adjacent outer doublets are connected by "nexin links" or "interdoublet links" which stretch from the A-tubule of one outer doublet to the B-tubule of the next outer doublet (Fig. 1*a*). The nexin links appear to occur throughout most of the length of the axoneme, and are spaced longitudinally at intervals of exactly four dynein arm repeats, or about 1,000 Å (see Fig. 4*e*). In longitudinal sections of axonemes, the nexin links sometimes have the appearance of a coiled or folded filament (Fig. 4*e*).

The A-tubule of each outer doublet is also connected to the B-tubule of the adjacent outer doublet by "peripheral links." The peripheral links differ from the nexin links in that they are prominent, densely staining structures limited to a region of the axoneme near its proximal end (see Figs. 10 and 13 in reference 41).

Radial spokes extend from the A-tubule of each outer doublet toward the center of the axoneme (Figs. 1 and 2*a*, *b*, *c*). Each radial spoke is about 385 Å in length and terminates in a bulbous enlargement, the "spoke head," which is about 80 Å in diameter. Longitudinally, the radial spokes are grouped together in pairs, which repeat at intervals of about 1,000 Å along the outer doublet; individual members of a pair are separated by a distance of about 274 Å, and pairs are separated by about 730 Å (Table I). The heads of the spokes in each pair appear to be connected by a thin fiber; this fiber is particularly prominent in negative stains (Fig. 2*c*, arrows).

The central tubules are surrounded by a "central sheath" which is composed of two pairs of projections, one pair extending from each central tubule (Fig. 1). In cross sections, the projections of one central tubule appear to be considerably shorter than the projections of the other central tubule; this is most readily seen in axonemes of mutant *pf-14* (Fig. 3*a*), where the absence of radial spokes (see below) permits a clearer image of the central sheath. The projections of the central tubules repeat longitudinally at intervals

FIGURE 1 Electron micrographs of isolated axonemes of wild-type *Chlamydomonas*. Fig. 1*a* Cross section in which the inner and outer dynein arms, the radial spokes, and the nexin links (arrows) are clearly visible. The central sheath is present but is difficult to distinguish from the spoke heads (compare with Fig. 3*a*). × 130,000. Fig. 1*b* Longitudinal section. One of the projections which make up the central sheath can be seen extending from the central tubule at intervals of 165 Å (arrows). The outer dynein arms (arrowheads) are evident along the outside edge of the left doublet microtubule, and the radial spokes (brackets) appear as paired projections extending from the outer doublets towards the central tubules. This axoneme bent to the right immediately below the region shown, and the "tilted spoke" configuration seen here may represent an initial stage in bend formation (see Warner and Satir [37]). × 160,000. Fig. 1*c* Longitudinal section. The radial spokes are grouped into pairs (brackets) which repeat at intervals of 1,000 Å. The inner dynein arms (arrows) are visible along the inner edge of the right doublet microtubule. × 130,000.

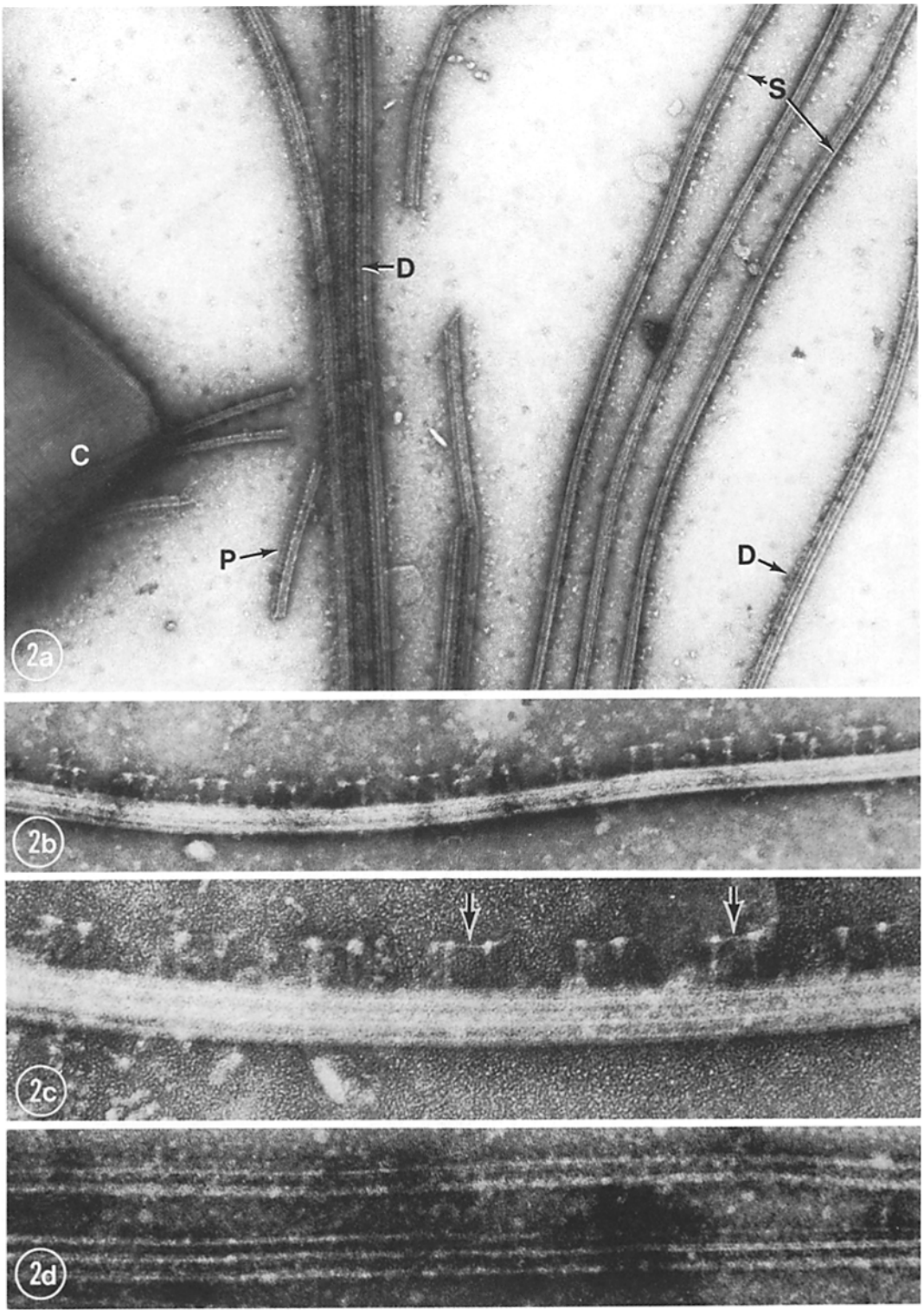
S
D
C
P
D
2a
2b
2c
2d

TABLE I

Axial Spacing of Axonemal Structures

Structure	Spacing	No. of 83 Å units
	Å	
Central sheath	165 ± 3*	2
Dynein arms	250 ± 5	3
Radial spokes		
S_1-S_2	274 ± 18	3.3
S_2-S_1	730 ± 16	8.8
S_1-S_1	1,004 ± 28	12
Nexin links	1,000	12

* Standard deviation.

of about 165 Å. The central tubules together with the central sheath will be referred to as the "central tubule-central sheath complex."

PF-14: Axonemes of this mutant appear to have structurally normal dynein arms, nexin links, and central tubule-central sheath complexes, but are missing the radial spokes (Figs. 2*d* and 3). As a result, the central tubule-central sheath complex appears to be free to move around within the ring of outer doublets, and is frequently located eccentrically (Fig. 3*a, b*). Because the spoke heads are absent, unobscured images of the central sheath can be obtained in cross sections of these axonemes; in such images the two long projections on one central tubule and the two short projections on the other central tubule are clearly visible (Fig. 3*a*). In many cross sections, the two central tubules appear to be linked by a bridge consisting of a pair of short rods; similar central tubule bridges have also been observed in mussel gill cilia (36) and rat sperm flagella (25).

PF-15A AND *PF-19*: Although mutants *pf*-15A and *pf-19* map to different linkage groups (12), the axonemes of the two mutants appear to be morphologically identical. In both, the dynein arms, nexin links, and radial spokes appear to be normal, but the central tubule-central sheath complex has been replaced by a densely staining core which runs longitudinally down the center of the axoneme (Figs. 4 and 5). This core is almost always present in intact flagella (42), but frequently diffuses away in demembranated axonemes, so that 80–90% of the axonemes are left with completely empty centers (Fig. 5*c, d*). In cross sections the core most frequently resembled a pair of globules (Fig. 5*a*) or a pair of dumbbells (Fig. 4*a*), but also commonly appeared as a hollow or solid cylinder, or as a hollow pentagon or hexagon with a large globule at each vertex. In longitudinal sections the cores frequently appeared structureless (Figs. 4*b* and 5*b*), but many cores showed hints of periodic cross-striations having a repeat of approximately 430 Å (Fig. 4*c*). These cross-striations were strongly reinforced when images of the cores were photographically translated one or two steps of the apparent repeat distance (Fig. 4*d*). Infrequently, one or both central tubules were observed in axonemes of both of these mutants; these observations are consistent with the report of Warr et al. (38) that mutants *pf-15A* and *pf-19* are slightly leaky.

Electrophoretic Analysis

When proteins of wild-type axonemes were analyzed by electrophoresis in SDS-acrylamide gels, the pattern shown in Fig. 6 (*WT*) was obtained. The major band *D* near the top of the gel represents dynein, and the major band *T* near the bottom of the gel represents tubulin, which is not resolved into its α- and β-subunits in this gel system. The gel also contains over 30 minor bands; for convenience of reference, these have been assigned numbers beginning with 1 for the uppermost band. The relative intensities and positions of these bands were reproducible from

FIGURE 2. Electron micrographs of negatively stained material. FIG. 2*a* Low-magnification view showing portions of a catalase crystal (*C*) and a disrupted axoneme of wild-type *Chlamydomonas*. Dynein arms (*D*) and radial spokes (*S*) are visible along several of the outer doublets, and central sheath projections (*P*) can be seen along a fragment of a central tubule. The lattice lines of the catalase crystal are clearly visible. × 49,000. Fig. 2*b* A wild-type outer doublet which has been tipped up on its edge so that the A- and B-tubules are superimposed. In this position the radial spokes are clearly seen as paired projections extending at right angles from the outer doublet. Some material appears to be present between the pairs of radial spokes, and probably represents the remains of the nexin links. × 113,000. Fig. 2*c* Higher magnification of a wild-type outer doublet. The heads of the spokes of each pair appear to be connected by a thin fiber (arrows). × 200,000. Fig. 2*d* Two outer doublets of mutant *pf-14*. Radial spokes have never been seen in negatively stained outer doublets of this mutant. × 150,000.

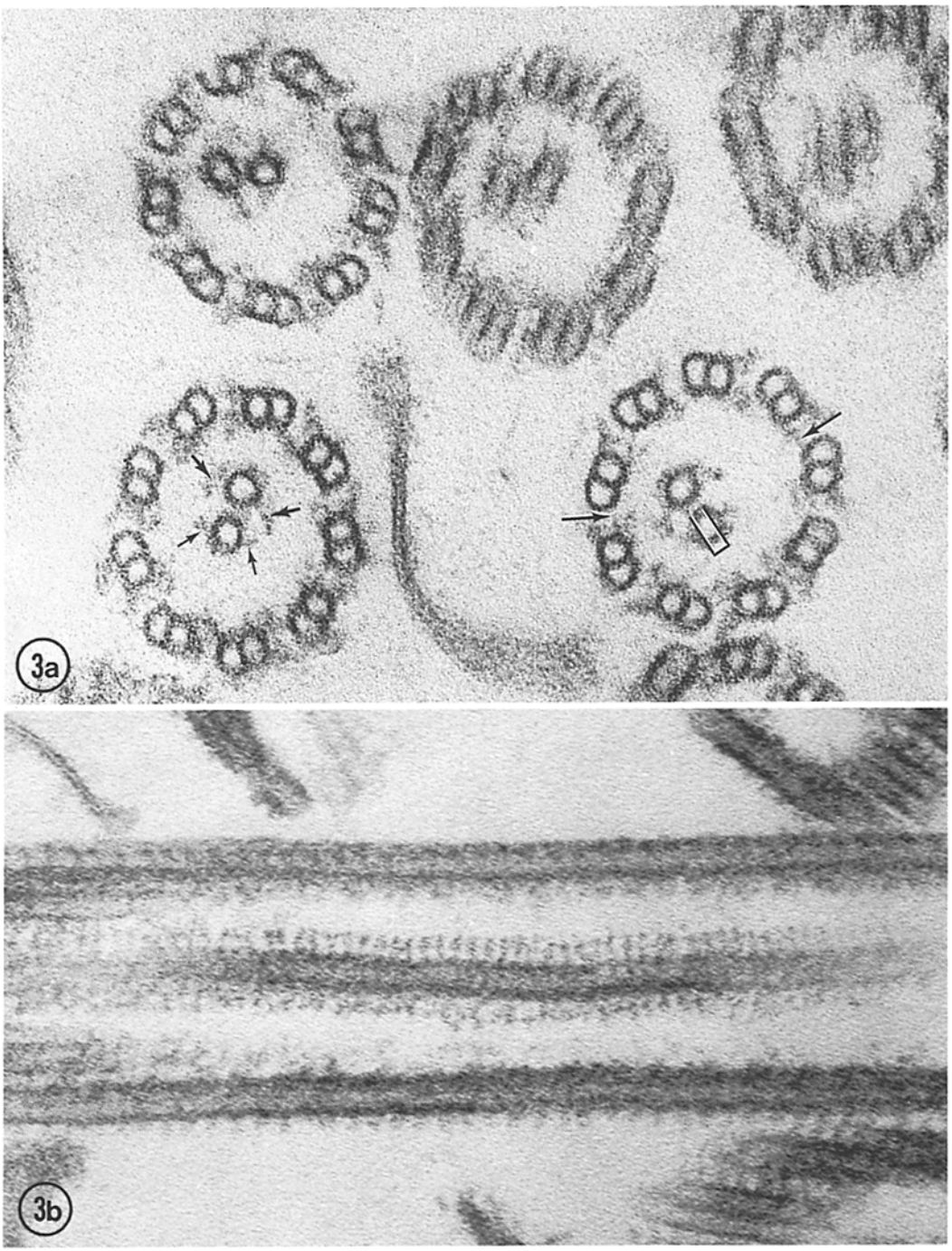

FIGURE 3 Electron micrographs of isolated axonemes of mutant *pf-14*. × 137,000. Fig. 3*a* In these cross sections, the arms of the outer doublets and the nexin links (arrows, lower right axoneme) appear morphologically normal, but there are no radial spokes, and the central tubule-central sheath complexes appear to be free to move around within the ring of outer doublets. In each axoneme, one central tubule has two long projections, and the other has two short projections (lower left axoneme, large and small arrows, respectively). In addition, the two central tubules often appear to be connected by a bipartite bridge (bracket). Fig. 3*b* A longitudinal section showing the complete absence of structured material between the outer doublets and the central tubule-central sheath complex. The central tubule-central sheath complex appears to meander along the axoneme in this mutant.

isolation to isolation and gel to gel. No sex-specific differences were observed when axonemal proteins of strains of opposite mating type were compared (results not shown).

A similar pattern was obtained when axonemes of the spokeless mutant *pf-14* were analyzed in the same gels (Fig. 6, label *14*). However, in gels of this mutant, band 21 was missing. Comparison of the relative mobility of this protein and those of proteins of known molecular weight indicated that it had a mol wt of about 118,000. This protein is presumably a component of the radial spokes.

Electrophoretic analyses of axonemal proteins of *pf-15A* and *pf-19* revealed that these mutants had abnormal levels of several proteins (Fig. 6, labels *15* and *19*, respectively). Bands 1, 7, and 13 appeared to be completely absent from gels of these strains, and the amount of protein in band 8 was usually present in reduced amounts compared to the wild-type level. In addition, protein 11 appeared to be present in elevated amounts compared to wild-type and *pf-14*. All these proteins appeared to be larger than 220,000 daltons; their precise molecular weights were not determined.

Reactivation

When wild-type axonemes were resuspended in HMDEKP containing 1 mM ATP, they began rapid beating with a highly asymmetrical wave form which caused them to swim rapidly around in a circle of relatively small radius (Fig. 7*a*). The form of the bending wave of these reactivating axonemes was virtually identical to that of *in situ* flagella of swimming cells; the frequency of beat (8–15 beats/s) was somewhat less than that of *in situ* flagella (20–25 beats/s, [Ray and Witman, manuscript in preparation]). With the dibucaine procedure for isolating axonemes, reactivation of 50–70% of the axonemes was common; in some preparations, virtually all of the axonemes reactivated. In one experiment, axonemes continued to beat on slides (with cover slips sealed with vaseline to prevent evaporation) for over 140 min. During this time there was no decrease in the percent of axonemes reactivating, but the beat frequency gradually slowed to zero, presumably as a result of depletion of ATP in the medium. Dibucaine-isolated axonemes still showed good reactivation after storage for several days in HMDEKP at 0°C.

In contrast, isolated axonemes of mutants *pf-14*, *pf-15A*, and *pf-19* could not be reactivated. Fig. 7*b* shows a multiple exposure, dark-field micrograph of axonemes of mutant *pf-14* under standard reactivating conditions. The axonemes remained intact but showed no active movement whatsoever. Similar results were obtained for axonemes of mutants *pf-15A* and *pf-19*.

ATP-Induced Disintegration of Axonemes

Summers and Gibbons (33) showed that when ATP was added to trypsin-treated axonemes of sea urchin sperm, the axonemes actively disintegrated as a result of interdoublet sliding. Allen and Borisy (3) recently reported that similar results could be obtained with *Chlamydomonas* axonemes, and we have used this technique to investigate whether axonemes of the mutants can undergo interdoublet sliding.

When wild-type axonemes were mixed with ATP and trypsin in HMDEKP and quickly examined by dark-field light microscopy, the axonemes were first observed to beat as under normal reactivating conditions, then to undergo a few seconds of uncoordinated twitching and bending, followed by rapid and synchronous disintegration. Most commonly, disintegrating axonemes frayed into thin strands which remained connected at one end, so that the resulting bundle of strands resembled a banana peel in shape (Fig. 8*a*). Alternatively, some axonemes disintegrated by elongating up to six times their original length, with a concomitant decrease in their brightness or apparent diameter; the long, thin strands resulting from this type of disintegration could often be seen to consist of slightly overlapping segments, each of which was about the length of the original axoneme (Fig. 8*b*). When disintegrated axonemes were negatively stained and examined by electron microscopy, the thin strands of the frayed axonemes were observed to be composed of single outer doublets or small groups of outer doublets; the longer strands of the elongated axonemes consisted of a series of individual outer doublets or pairs of outer doublets joined together over short regions of overlap. Both axonemal fraying and elongation required ATP; neither type of disintegration occurred in the presence of trypsin without ATP. Both fraying and elongation must therefore be due to ATP-induced sliding of outer doublets.

When axonemes of mutants *pf-14*, *pf-15A*, and *pf-19* in HMDEKP were mixed with ATP and trypsin, the axonemes were observed to be ini-

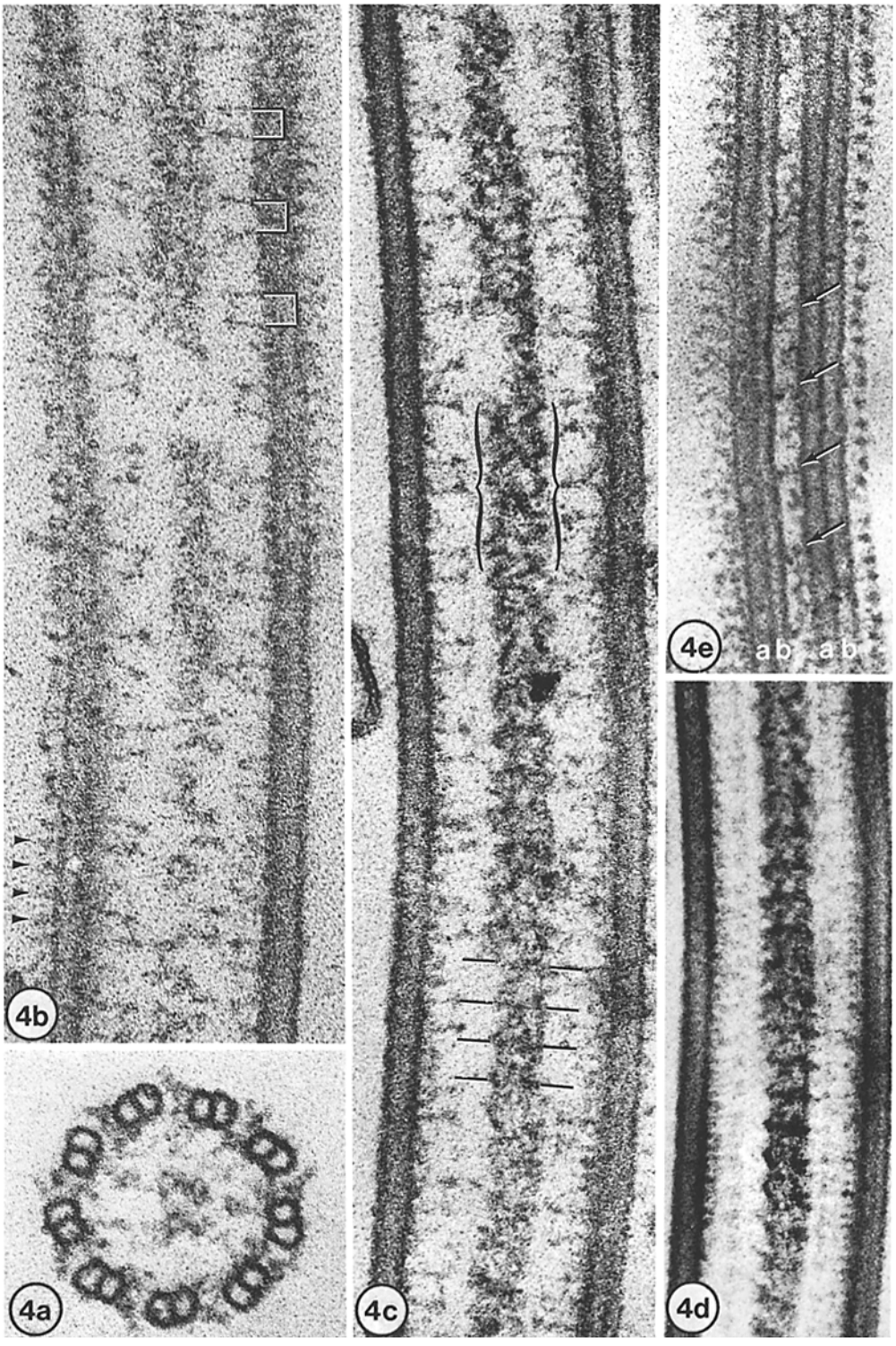
4b
4a
4c
4e
a b a b
4d

tially motionless, then to undergo a brief period of twitching, and finally to disintegrate in the same manner as wild-type axonemes. Fig. 8*c* is a dark-field light micrograph of isolated axonemes of mutant *pf-19* after ATP-induced disintegration; several of the axonemes have frayed apart, and at least one (arrow) has disintegrated by elongation. Similar results were obtained with axonemes of *pf-14* and *pf-15A*. As with wild type, no disintegration occurred in the presence of trypsin without ATP. These results indicated that ATP-induced sliding of outer doublets could occur in all three mutants.

A semiquantitative measure of the rate and the total amount of ATP-induced disintegration in a preparation of axonemes can be obtained by following the decrease in turbidity (A_{350}) of axonemal suspensions after addition of ATP and trypsin (34). Wild-type *Chlamydomonas* axonemes in HMDEKP and 0.1 mM ATP alone showed very little decrease in turbidity with increasing time (see Fig. 9*a*). When trypsin but no ATP was added to the suspensions, the turbidity decreased at a moderate and fairly constant rate. This drop was due to the progressive digestion of the axonemes by trypsin (34). In contrast, addition of 0.1 mM ATP and trypsin together resulted in a very rapid drop in the turbidity of the suspension to about one-half of its initial value; this drop was nearly complete within 2 min, and was followed by a much slower decrease similar to that observed in the presence of tryspin alone. Light and electron microscope examination of such suspensions indicated that the rapid drop was due to disintegration of the axonemes, as described above. A similar drop was observed when ATP was added after several minutes of digestion with trypsin (Fig. 9*a*), or after trypsin digestion which had been previously terminated by addition of soybean trypsin inhibitor (not shown). These latter results indicated that the final turbidity reached as a result of ATP-induced disintegration was relatively insensitive to the amount of axonemal digestion that had occurred.

When the trypsin-plus-ATP-induced disintegrations of axonemes of mutants *pf-14*, *pf-15A*, and *pf-19* were monitored by spectrophotometry (see Fig. 9*b*, *c*, and *d*, respectively), results similar to those described above for wild type were obtained. Suspensions of axonemes of all three mutants underwent a precipitous drop in turbidity to about one-half of their initial values after addition of trypsin in the presence of 0.1 mM ATP; this decrease occurred at approximately the same rate as that of wild type, and, like wild type, was complete within 2 min. A rapid decrease in turbidity was also observed when ATP was added after several minutes of digestion with trypsin. ATP alone usually caused no change in turbidity, whereas trypsin alone caused a moderate decrease. These results indicated that both the average rate of disintegration and the total amount of disintegration were the same in axonemes of wild type and the three mutants.

FIGURE 4 Electron micrographs of isolated axonemes of mutant *pf-15A*. Fig. 4*a* Cross section. The central tubule-central sheath complex is absent and has been replaced by a core which in cross section resembles a pair of dumbbells. The dynein arms, radial spokes, and nexin links appear normal. × 137,000. Fig. 4*b* Longitudinal section. The core replacing the central tubule-central sheath complex runs longitudinally down the center of the axoneme and here has no apparent fine structure. The radial spokes (brackets) and outer dynein arms (arrowheads) are visible and have normal spacing and appearance. × 137,000. Fig. 4*c* Longitudinal section through an axoneme in which a region of the core appears to have faint cross-striations (bars) repeating at intervals of about 430 Å. Farther along the axoneme the core has a herringbone appearance (braces). × 133,000. Fig. 4*d* A photographic translation of the lower two-thirds of the micrograph shown in Fig. 4*c*. The micrograph was translated twice in steps of the apparent repeat distance of the cross-striations of the central core. Electron-dense regions are strongly reinforced the entire length of the core. (Reduced to 4/5 from Fig. 4*c*). Fig. 4*e* Longitudinal section through two adjacent outer doublets. The nexin links (arrows) connect the A-tubule of the right outer doublet to the B-tubule of the left outer doublet at 1,000 Å intervals. These links are tilted at angles of 30–40° from a line perpendicular to the outer doublets, and some have the appearance of a coiled or folded filament (second arrow from bottom). The dynein arms of the outer doublet on the left can be seen extending from the edge of its A-tubule; the row of dots to the right of the right outer doublet are the outer arms of a third doublet (just out of the section) which have been cut transversely. *a*, *b*, A- and B-tubules of the outer doublets. × 122,000.

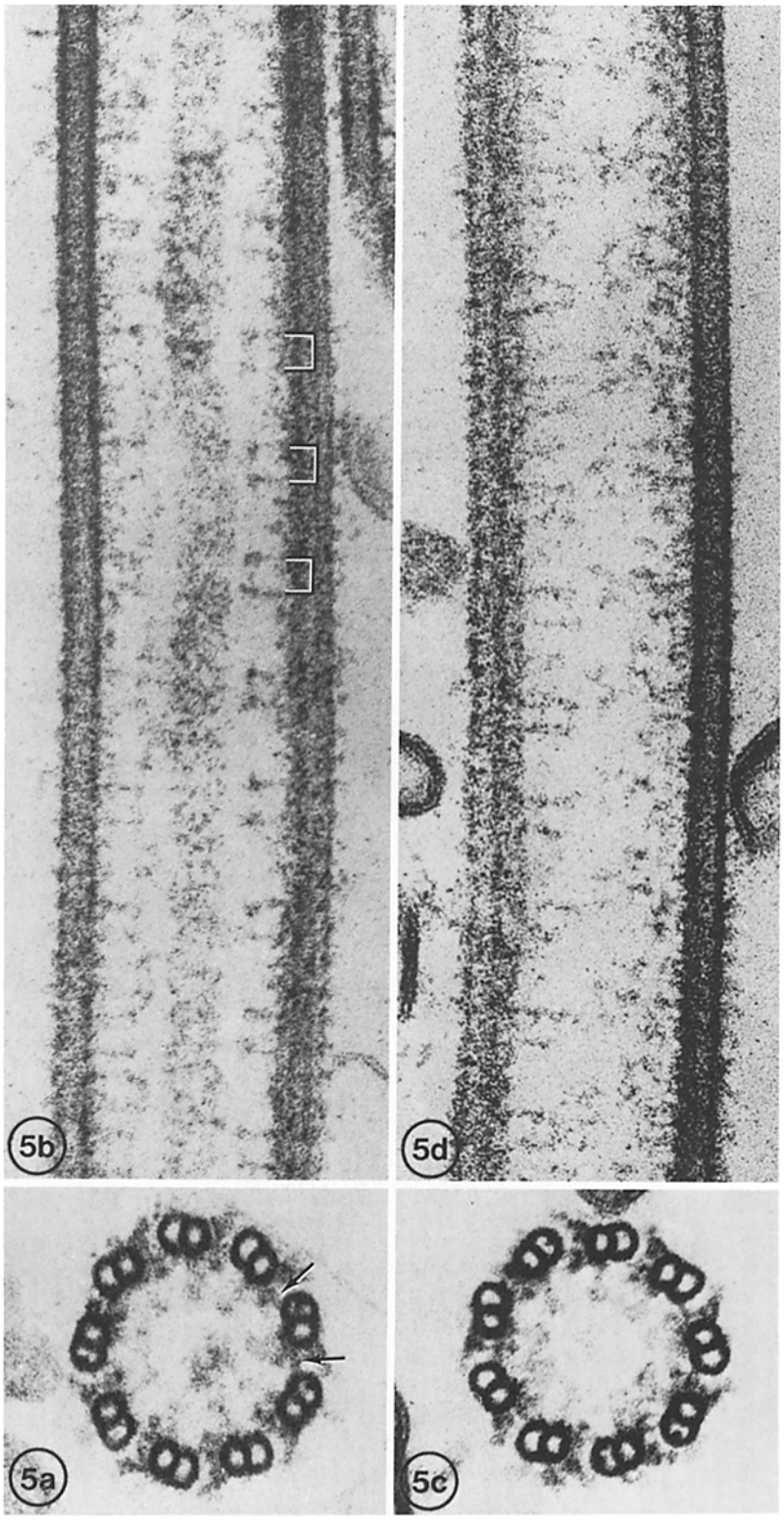

FIGURE 5 Electron micrographs of isolated axonemes of mutant *pf-19*. × 150,000. Fig. 5*a* and *b*. As in mutant *pf-15A*, the central tubule-central sheath complex has been replaced by a core which runs longitudinally down the center of the axoneme. The inner and outer dynein arms, the radial spokes (brackets), and the nexin links (arrows) appear normal. Fig. 5*c* and *d*. Axonemes of mutant *pf-19* in which the central core has diffused away, leaving a hollow ring of doublet microtubules.

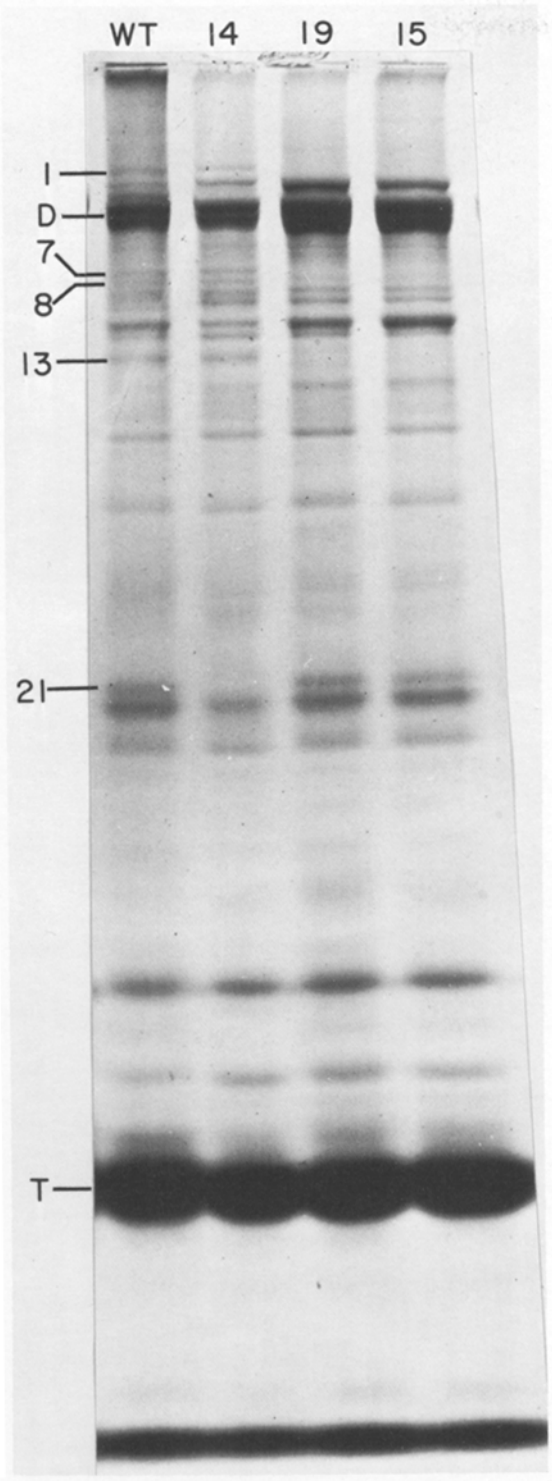

FIGURE 6 SDS-acrylamide slab gel of isolated axonemes of wild-type (*WT*) and mutants *pf-14*, *pf-19*, and *pf-15A* (*14*, *19*, and *15*, respectively). *D* and *T* indicate dynein and tubulin bands, respectively; for convenience of reference, other bands are assigned numbers beginning with 1 at the top of the gel. In *pf-14*, band 21 is absent. In *pf-19* and *pf-15A*, bands 1, 8, and 13 are absent, band 7 is present in reduced amounts, and band 11 (not marked) is elevated.

DISCUSSION

Fine Structure

Electron microscope examination of both thin-sectioned and negatively stained axonemes of mutant *pf-14* clearly indicated that this mutant lacks the radial spokes. These observations confirm previous reports on the fine structure of this mutant (26, 42). It should be emphasized that, in addition to having apparently normal dynein arms and central tubule-central sheath complexes, *pf-14* appears to have structurally normal nexin links. This is important in differentiating between the functions of the radial spokes and the nexin links (see below).

As previously reported (38, 42), mutants *pf-15A* and *pf-19* are missing the central tubules and their associated sheath, which have been replaced by a core which runs longitudinally down the center of the axoneme. In both mutants, the cores frequently have periodic cross-striations spaced about 430 Å apart. This spacing is not simply related to that of the radial spokes or the central sheath, but could have a vernier relationship to the period of the latter structure.

Our observations on axonemes of both wild-type and mutant *Chlamydomonas* indicate that the nexin links extend from the A-tubule of one outer doublet to the B-tubule of the adjacent outer doublet, and repeat longitudinally at intervals of about 1,000 Å. This is in good agreement with the reports of Allen (4) and Williams and Luft (39) that a thin fiber extends from the A-tubule of one outer doublet to the B-tubule of the adjacent outer doublet in *Tetrahymena* cilia, and of Warner (36), who clearly showed A- to B-tubule links occurring at intervals of about 860 Å along the outer doublets of mussel gill cilia. Similarly, Dallai et al. (11) observed thin A- to B-tubule connections spaced about 950 Å apart along the doublets of the flagellar complex of *Sciara*. There have been some reports that the nexin links connect adjacent A-tubules (14, 32), but these reports may have been in error. Gibbons (14) reported "a line . . . joining adjacent A subfi-

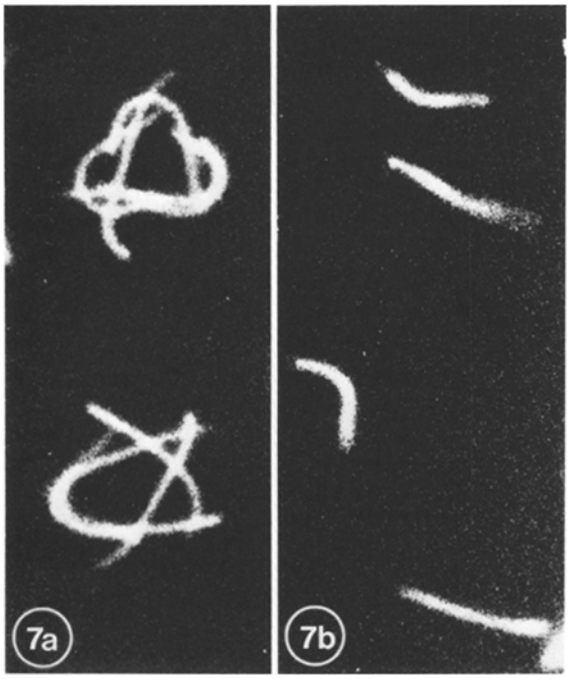

FIGURE 7 Multiple flash, dark-field light micrographs of two axonemes of wild-type (Fig. 7*a*) and four axonemes of mutant *pf-14* (Fig. 7*b*) under reactivating conditions. The wild-type axonemes are beating with a highly asymmetric bend which causes them to swim in a circle of relatively small radius; axonemes of mutant *pf-14*, under identical conditions, show no active movements. Flash rate 10 Hz; 1/2 s exposure. × 2,980.

bers" in *Tetrahymena*, but on close examination of his published micrographs (Figs. 3, 6, and 19 in reference 14), this line actually appears to join the A-tubule of each outer doublet with the B-tubule of the adjacent outer doublet, as described by Allen (4) and Williams and Luft (39) for *Tetrahymena*. Stephens (32) presented evidence that in echinoderm sperm flagella the nexin links connect adjacent A-tubules: when the B-tubules of isolated axonemes were depolymerized, the remaining A-tubules appeared to still be connected by bridges repeating at intervals of about 1,000 Å along the outer doublets. However, more recent work has suggested other interpretations of Stephens' observations. When the B-tubules of *Chlamydomonas* axonemes were selectively solubilized, the cylindrical arrangement of the A-tubules persisted, even though no intact nexin links were apparent in thin section (see Fig. 15 in reference 41; the A-tubules appear to be held together by a web of fibrous material). If a similar situation occurred in Stephens' experiments, the A-tubules may not have been specifically bound together by nexin links, and the periodic "bridge" observed by Stephens may actually have been clumped radial spokes, as suggested by Warner (36), or nexin links which remained connected to the A-tubule at one end but were no longer specifically bound at their other end. Moreover, in thin sections of sea urchin sperm axonemes, the nexin links very clearly appear to join the A-tubule of one outer doublet with the B-tubule of the adjacent outer doublet (e.g., see Figs. 4, 5, and 9 in reference 15). The available evidence therefore strongly suggests that an A- to B-tubule connection may be a common feature of all interdoublet links.

Several investigators have previously reported that the radial spokes are grouped together in pairs in *Chlamydomonas* (2, 10, 16, 24). However, recent findings that the radial spokes are arranged in triplets in *Tetrahymena* cilia (9) and mussel gill cilia (37) have prompted some investigators to suggest that a triplet grouping may be a feature common to all "9+2" flagella, and that the apparent pairing of spokes in *Chlamydomonas* may have been an artifact resulting from loss of the third spoke during specimen preparation (9, 10, 37). This argument was supported by Chasey's observation of dense "spots" lying between spoke pairs of *Chlamydomonas* outer doublets (10); Chasey proposed that these spots, spaced at 1,000 Å intervals, represented the remains of a third spoke. However, in the present study we also have observed pairs of spokes in *Chlamydomonas*, and several considerations suggest that such a grouping actually is representative of the in vivo arrangement of the spokes: (*a*) inasmuch as the isolated axonemes could be reactivated, it seems unlikely that the third spoke was lost before preparation for electron microscopy; (*b*) it is improbable that a third spoke would have been lost consistently in both thin-sectioned and negatively stained material; and (*c*) the triplet grouping of spokes in *Tetrahymena* was well preserved by the same methods of preparation (Eisler and Witman, unpublished observations). Furthermore, we have found that the nexin links repeat longitudinally at intervals of 1,000 Å in *Chlamydomonas*, suggesting that the dense spots observed by Chasey were actually nexin links which collapsed back onto the A-tubule after the axoneme frayed apart. Although the existence of a third spoke in *Chlamydomonas* cannot be absolutely ruled out on the

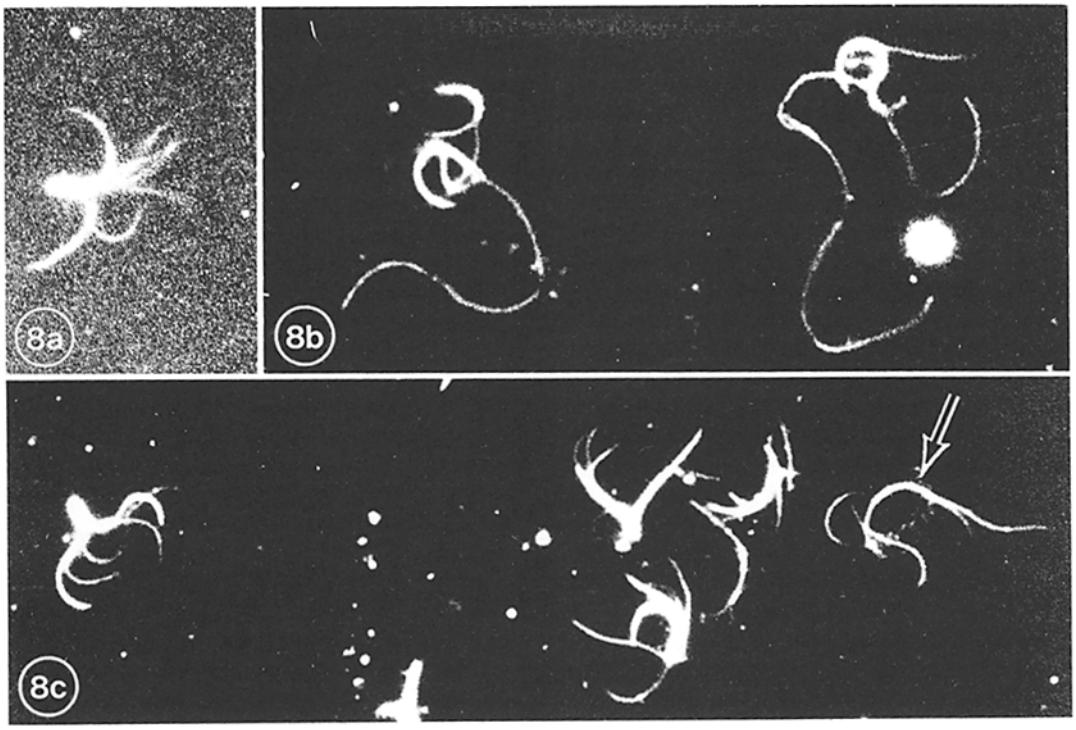

FIGURE 8 Dark-field light micrographs of isolated axonemes after treatment with trypsin in the presence of ATP. Fig. 8*a* A wild-type axoneme which has frayed into a number of thin strands which remain joined together at one end. × 2,140. Fig. 8*b* Two wild-type axonemes which have disintegrated by elongation. In the axoneme on the right the long thin strands appear to be composed of a number of overlapping segments. × 1,920. Fig. 8*c* Several axonemes of mutant *pf-19* which have disintegrated by fraying, and at least one (arrow) which has disintegrated by elongation. × 1,870.

basis of the above findings, the evidence strongly suggests that the spokes do occur in pairs in this organism. If a third spoke does exist, it must differ greatly from the other two spokes in its solubility or lability.

Examination of the central sheath in thin-sectioned axonemes of wild type, and particularly *pf-14*, where it is possible to obtain unobstructed images of the central tubules, indicated that in *Chlamydomonas* one central tubule has two relatively long projections and the other has two shorter projections. Hopkins (16) previously reported that in *Chlamydomonas* one central tubule had two projections and the other had one, slightly shorter, projection; however, Hopkins' observations were made on negatively stained material in which the second short projection may have been concealed or solubilized. This central sheath asymmetry could result in modified radial spoke-central sheath interactions (see below) in opposite halves of the axoneme, leading to the asymmetrical beat observed in *Chlamydomonas* flagella during normal forward swimming (28). Interestingly, the central sheath has been reported to be asymmetrical in cilia and flagella of several other organisms, including *Tetrahymena* (4, 8, 39), rat sperm (25), the ctenophore *Mnemiopsis* (1), and the fresh water mussel *Anodonta* (13), and in all these species the cilia or flagella have a highly asymmetrical beat.

Using the lattice spacing of crystalline catalase as an internal standard, we have obtained accurate measurements for the longitudinal spacing of the various axonemal components. These measurements indicated that the projections of the central tubules, the dynein arms, the nexin links, and the pairs of radial spokes repeat at intervals of 2, 3, 12, and 12 times 83 Å, respectively (see Table I). This 83 Å common denominator probably corresponds to the axial repeat of the tubulin dimer in *Chlamydomonas*. Our findings are therefore in good agreement with the findings of McIntosh

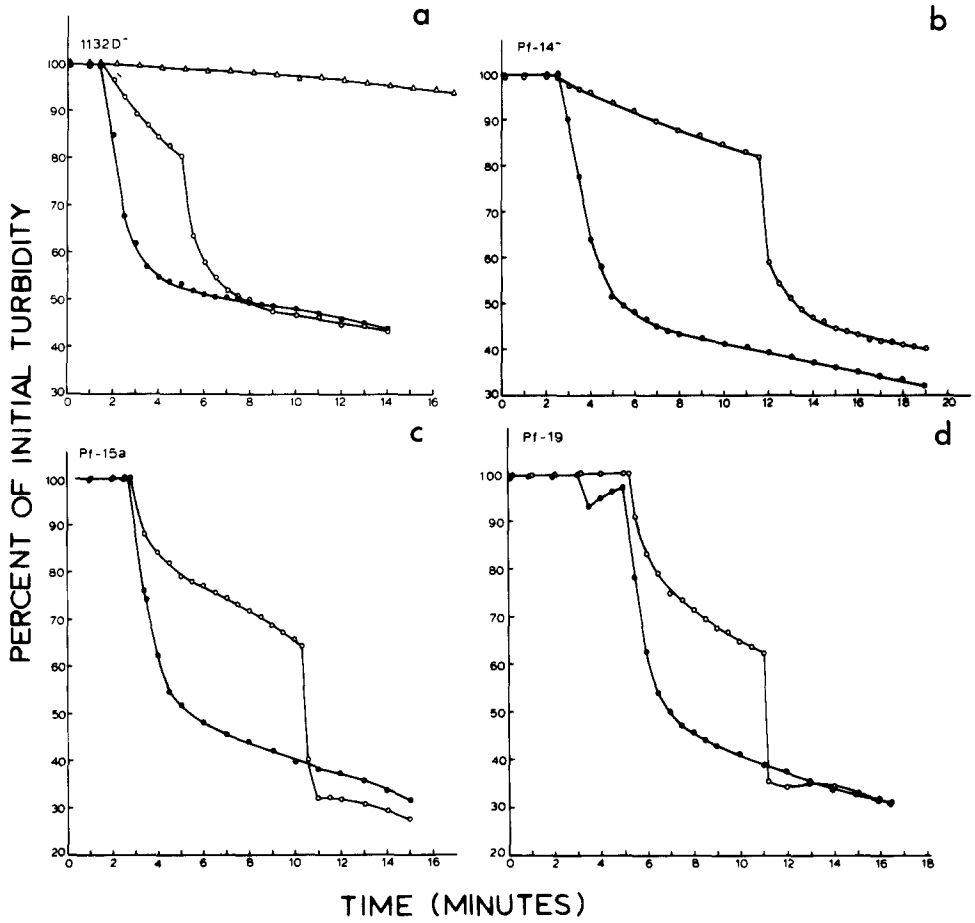

FIGURE 9 Change in turbidity (A_{350}) vs. time for suspensions of isolated axonemes in HMDEKP with or without trypsin and ATP. Fig. 9*a* Wild-type axonemes: (●) trypsin and ATP added at 1.5 min; (○) trypsin alone added at 1.5 min, ATP added at 5 min; (△) ATP alone added at 1.5 min. Fig. 9*b* *Pf-14* axonemes: (●) trypsin and ATP added at 2.5 min; (○) trypsin alone added at 2.5 min, ATP added at 11.5 min. Fig. 9*c* *Pf-15A* axonemes: (●) trypsin and ATP added at 3 min; (○) trypsin alone added at 3 min, ATP added at 10 min. Fig. 9*d* *Pf-19* axonemes: (●) ATP added at 3 min, trypsin added at 5 min (a transient drop in turbidity was occasionally observed upon addition of ATP alone, regardless of the type of axonemes); (○) trypsin added at 5 min, ATP added at 11 min.

(23) and Amos et al. (5) that the flagellar components are spaced at integral multiples of the tubulin dimer spacing. The 274 and 730 Å intervals between alternate radial spokes in *Chlamydomonas* do not fit into this pattern, but considerable variation was present in these measurements, and these values may be in error. Further study will therefore be necessary to determine with certainty whether or not the spacing of the paired spokes of *Chlamydomonas* is directly related to the outer doublet surface lattice.

Protein Composition

SDS-acrylamide gel electrophoresis of isolated, reactivatable, wild-type axonemes indicated that they contained over 30 proteins in addition to the dyneins and tubulins. Because these axonemes were demembranated, any soluble "matrix" proteins should have been removed in the washes, so that the proteins remaining were presumably structural components of the axoneme. One of these proteins, having a mol wt of about 118,000, is missing in axonemes of the spokeless mutant *pf-14;* this protein must represent a major component of the radial spokes. However, a radial spoke appears to be too large and too complex a structure to be composed of a single protein of this size; assuming a protein density of about 1.3

g/cm^3, the approximate molecular weight of a spoke composed of a 40 × 300 Å cylindrical shaft capped by a globule 80 Å in diameter would be about 500,000. The radial spokes therefore probably contain other proteins not resolved in our gel system. Recently, Piperno et al. (26), using a two-dimensional isoelectric focusing and SDS-gel electrophoresis system, reported that axonemes of mutant *pf-14* were missing 12 proteins (total mol wt: 729,000) out of a total of 130 polypeptides present in wild-type axonemes; this seems a more reasonable estimate of the total number and molecular weight of the radial spoke proteins. The results of Piperno et al. also indicate that the *Chlamydomonas* axoneme probably contains many more structural proteins than were detected in our gel system.

In the present study, three proteins having molecular weights greater than 220,000 were found to be missing in axonemes of the central tubuleless mutants *pf-15A* and *pf-19*. These proteins are probably components of the central sheath or the bridge between the two central tubules. A third protein (band 8 in Fig. 6) was present in varying but usually reduced amounts compared to its wild-type levels. Inasmuch as the central core was removed from a varying percentage of these axonemes in different preparations, band 8 may represent a component of the central tubule-central sheath complex which was incorporated into the core.

Olson and Linck (25) recently reported the isolation of the central tubule-central sheath complex from squid sperm flagella. In SDS-acrylamide gels of these complexes, there does not appear to be a great enrichment for any high molecular weight proteins which might correspond to the central tubule-central sheath proteins identified in the present study. Although this could be due to species differences, it is also possible that the proteins of the squid sperm complex were digested by sperm proteases during the isolation procedure. We are presently attempting to isolate the central tubule-central sheath complex from *Chlamydomonas;* because preparations of *Chlamydomonas* axonemes appear to be free of protease activity, the composition of the complex could be determined directly without risk of proteolysis of the protein components.

Function of the Radial Spokes and Central Tubule-Central Sheath Complex

When wild-type axonemes were reactivated, they beat in a manner similar to that of *in situ* flagella of swimming cells. In contrast, axonemes of mutants *pf-14, pf-15A,* and *pf-19* could not be reactivated. However, axonemes of these mutants did disintegrate as a result of ATP-induced interdoublet sliding after brief digestion with trypsin, and both the rate of sliding and the total amount of sliding were the same in preparations of axonemes from all three mutants as from wild type. These results indicated that the dynein arms were functional in the mutants and could generate interdoublet shearing forces.

The fact that axonemes of the mutants could undergo interdoublet sliding but could not be reactivated indicates that the radial spokes and the central tubule-central sheath complex are both necessary for the conversion of microtubule sliding into axonemal bending. This is in good agreement with the observations of Warner and Satir (37) on radial spoke configurations in mussel gill cilia. Warner and Satir found that the radial spokes were attached to the central sheath in bent regions of the axoneme, but were functionally detached in straight regions. They concluded that radial spoke-central sheath interactions are part of the mechanism for converting active outer doublet sliding into axonemal bending. Our findings that both the radial spokes and the central tubule-central sheath complex are necessary for this conversion now provide strong support for Warner and Satir's hypothesis. Further studies will be necessary to determine how the radial spokes and the central sheath interact, and how these interactions are controlled to give rise to coordinated flagellar movement.

Function of Nexin Links

Our observations on mutant *pf-14* also provide information on the specific roles of the nexin links. In their studies on interdoublet sliding in trypsin-treated axonemes of sea urchin sperm, Summers and Gibbons (34) found that the radial spokes and the nexin links were disrupted at about the same time as the axoneme became susceptible to ATP-induced disintegration. They concluded that one or both of these structures was responsible for limiting the amount of sliding which occurred between outer doublets in the intact axonemes. However, because the radial spokes and the nexin links were digested at the same rate, nothing could be concluded about the individual roles of either component. In the present study, we observed that nontrypsinized axo-

nemes of *pf-14* remained intact in the presence of ATP. Because axonemes of this mutant lack the radial spokes but have intact nexin links, the nexin links alone must be capable of maintaining the structural integrity of the axoneme against dynein-generated shearing forces. The nexin links must therefore form permanent bridges between adjacent outer doublets; otherwise, axonemes of mutant *pf-14* would disintegrate under reactivating conditions. This finding is in good agreement with the ultrastructural observation that, in longitudinal sections of axonemes, the nexin links are often inclined from a line perpendicular to the outer doublets (Fig. 4*e* and reference 36), as would be expected if the links were permanently bonded to the outer doublets and were pulled axially during interdoublet sliding.

Certain predictions can be made about the role of a permanently attached interdoublet link in the control of flagellar wave form. According to the sliding filament model, the angle subtended by a flagellar bend is directly related to the amount of sliding that occurs between axonemal microtubules (30). Assuming that the nexin links are elastic (25, 36) and stretch to accommodate sliding displacement between adjacent outer doublets, the maximum amount of sliding that can occur under any conditions will be limited by the elasticity of the nexin links. This will then set an upper limit on the size of the bend angle that can be formed. In flagella beating at submaximum bend angles, the nexin links would still be expected to make a significant contribution to the internal elastic resistance of the flagellum. If bend angle is determined by a balance between elastic resistance and active bending forces (7), then the nexin links will have an important role in determining the bend angle.

Functions of the Peripheral Links

The observations on ATP-induced axonemal disintegration in *Chlamydomonas* also suggest a possible role for the peripheral links. Trypsin-treated axonemes of both wild-type and mutant *Chlamydomonas* most commonly underwent a type of disintegration in which the outer doublets remained connected at one end. This was the proximal end, because isolated axonemes are often slightly frayed apart at their distal ends even in the absence of trypsin treatment (2, 40). Isolated axonemes of *Chlamydomonas* do not retain their basal bodies, but the outer doublets are linked together proximally by the peripheral links (41). It is probably these peripheral links that held the outer doublets together after axonemal disintegration. Because these links can apparently resist interdoublet shearing forces, even after digestion of the nexin links, their function in the intact axoneme is probably to tie the outer doublets firmly together at their proximal ends, thus preventing sliding displacements between microtubules in the proximal region of the axoneme.

This study was supported by a grant from The Whitehall Foundation and by National Institutes of Health grant GM 21586 awarded to George Witman.

Received for publication 6 September 1977, and in revised form 14 November 1977.

REFERENCES

1. AFZELIUS, B. 1961. The fine structure of the cilia from ctenophore swimming plate. *J. Biophys. Biochem. Cytol.* **9**:383–394.
2. ALLEN, C., and G. G. BORISY. 1974. Structural polarity and directional growth of microtubules of *Chlamydomonas* flagella. *J. Mol. Biol.* **90**:381–402.
3. ALLEN, C., and G. G. BORISY. 1974. Flagellar motility in *Chlamydomonas:* reactivation and sliding in vitro. *J. Cell Biol.* **63**:5*a* (Abstr).
4. ALLEN, R. D. 1968. A reinvestigation of cross-sections of cilia. *J. Cell Biol.* **37**:825–831.
5. AMOS, L. A., R. W. LINCK, and A. KLUG. 1976. Molecular structure of flagellar microtubules. *In* Cell Motility. R. D. Goldman, T. D. Pollard, and J. L. Rosenbaum, editors. Cold Spring Harbor Laboratory, Cold Spring Harbor, N. Y. 847–867.
6. BROKAW, C. J. 1972. Flagellar movement: a sliding filament model. *Science (Wash. D. C.).* **178**:455–462.
7. BROKAW, C. J. 1975. Effects of viscosity and ATP concentration on the movement of reactivated sea urchin sperm flagella. *J. Exp. Biol.* **62**:701–719.
8. CHASEY, D. 1969. Observations on the central pair of microtubules from the cilia of *Tetrahymena pyriformis*. *J. Cell Sci.* **5**:453–458.
9. CHASEY, D. 1972. Further observations on the ultrastructure of cilia from *Tetrahymena pyriformis*. *Exp. Cell Res.* **74**:471–479.
10. CHASEY, D. 1974. The three-dimensional arrangement of radial spokes in the flagella of *Chlamydomonas reinhardii*. *Exp. Cell Res.* **84**:374–380.
11. DALLAI, R., F. BERNINI, and G. GIUSTI. 1973. Interdoublet connections in the sperm flagellar complex of *Sciara*. *J. Submicrosc. Cytol.* **5**:137–145.
12. EBERSOLD, W. T., R. P. LEVINE, E. E. LEVINE, and M. A. OLMSTED. 1962. Linkage maps in *Chlamydomonas reinhardii*. *Genetics.* **47**:531–543.
13. GIBBONS, I. R. 1961. The relationship between the

fine structure and direction of beat in gill cilia of a lamellibranch mollusc. *J. Biophys. Biochem. Cytol.* **11**:179.

14. GIBBONS, I. R. 1965. Chemical dissection of cilia. *Arch. Biol.* **76**:317–352.
15. GIBBONS, B. H., and I. R. GIBBONS. 1973. The effect of partial extraction of dynein arms on the movement of reactivated sea urchin sperm. *J. Cell Sci.* **13**:337–357.
16. HOPKINS, J. M. 1970. Subsidiary components of the flagella of *Chlamydomonas reinhardii*. *J. Cell Sci.* **7**:823–839.
17. LAEMMLI, U. K. 1970. Cleavage of structural proteins during the assembly of the head of the bacteriophage T4. *Nature (Lond.)*. **227**:680–685.
18. LAEMMLI, U. K., and M. FAVRE. 1973. Maturation of the head of bacteriophage T4. I. DNA packaging events. *J. Mol. Biol.* **80**:575–599.
19. LEWIN, R. A. 1974. Genetic control of flagellar activity in *Chlamydomonas moewusii* (Chlorophyta, Volvocales). *Phycologia.* **13**:45–55.
20. LOWRY, O. H., N. J. ROSEBROUGH, A. L. FARR, and R. J. RANDALL. 1951. Protein measurement with the Folin phenol reagent. *J. Biol. Chem.* **193**:265–275.
21. LUFT, J. H. 1961. Improvements in epoxy resin embedding methods. *J. Biophys. Biochem. Cytol.* **9**:409–414.
22. LUFTIG, R. 1967. An accurate measurement of the catalase crystal period and its use as an internal marker for electron microscopy. *J. Ultrastruct. Res.* **20**:91–102.
23. MCINTOSH, J. R. 1974. Bridges between microtubules. *J. Cell Biol.* **61**:166–187.
24. MCVITTIE, A. 1972. Flagellum mutants of *Chlamydomonas reinhardii*. *J. Gen. Microbiol.* **71**:525–540.
25. OLSON, G. E., and R. W. LINCK. 1977. Observations on the structural components of flagellar axonemes and central pair microtubules from rat sperm. *J. Ultrastruct. Res.* **61**:21–43.
26. PIPERNO, G., B. HUANG, and D. J. L. LUCK. 1977. Two-dimensional analysis of flagellar proteins from wild-type and paralyzed mutants of *Chlamydomonas reinhardii*. *Proc. Natl. Acad. Sci. U. S. A.* **74**:1600–1604.
27. REYNOLDS, E. 1963. The use of lead citrate at high pH as an electro-opaque stain in electron microscopy. *J. Cell Biol.* **17**:208–212.
28. RINGO, D. L. 1967. Flagellar motion and fine structure of the flagellar apparatus in *Chlamydomonas*. *J. Cell Biol.* **33**:543–571.
29. SAGER, R., and S. GRANICK. 1953. Nutritional studies with *Chlamydomonas reinhardii*. *Ann. N. Y. Acad. Sci.* **56**:831–838.
30. SATIR, P. 1968. Studies on cilia. III. Further studies on the cilium tip and a "sliding filament" model of ciliary motility. *J. Cell Biol.* **39**:77–94.
31. SATIR, P. 1974. The present status of the sliding microtubule model of ciliary motion. *In* Cilia and Flagella. M. A. Sleigh, editor. Academic Press, Inc., New York. 131–142.
32. STEPHENS, R., E. 1970. Isolation of nexin - the linkage protein responsible for maintenance of the nine-fold configuration of flagellar axonemes. *Biol. Bull. (Woods Hole).* **139**:438.
33. SUMMERS, K. E., and I. R. GIBBONS. 1971. Adenosine triphosphate-induced sliding of tubules in trypsin-treated flagella of sea urchin sperm. *Proc. Natl. Acad. Sci. U. S. A.* **68**:3092–3096.
34. SUMMERS, K. E., and I. R. GIBBONS. 1973. Effects of trypsin digestion on flagellar structures and their relationship to motility. *J. Cell Biol.* **58**:618–629.
35. THOMPSON, G. A., JR., L. C. BAUGH, and L. F. WALKER. 1974. Nonlethal deciliation of *Tetrahymena* by a local anesthetic and its utility as a tool for studying cilia regeneration. *J. Cell Biol.* **61**:253–257.
36. WARNER, F. D. 1976. Ciliary inter-microtubule bridges. *J. Cell Sci.* **20**:101–114.
37. WARNER, F. D., and P. SATIR. 1974. The structural basis of ciliary bend formation. Radial spoke positional changes accompanying microtubule sliding. *J. Cell Biol.* **63**:35–63.
38. WARR, J. R., A. MCVITTAE, J. RANDALL, and J. M. HOPKINS. 1966. Genetic control of flagellar structure in *Chlamydomonas reinhardii*. *Genet. Res.* **7**:335–351.
39. WILLIAMS, N. E., and J. H. LUFT. 1968. Use of a nitrogen mustard derivative in fixation for electron microscopy and observations on the ultrastructure of *Tetrahymena*. *J. Ultrastruct. Res.* **25**:271–292.
40. WITMAN, G. B. 1975. The site of *in vivo* assembly of flagellar microtubules. *Ann. N. Y. Acad. Sci.* **253**:178–191.
41. WITMAN, G. B., K. CARLSON, J. BERLINER, and J. L. ROSENBAUM. 1972. *Chlamydomonas* flagella. I. Isolation and electrophoretic analysis of microtubules, matrix, membranes, and mastigonemes. *J. Cell Biol.* **54**:507–539.
42. WITMAN, G. B., R. FAY, and J. PLUMMER. 1976. *Chlamydomonas* mutants: evidence for the roles of specific axonemal components in flagellar movement. *In* Cell Motility. R. D. Goldman, T. D. Pollard, and J. L. Rosenbaum, editors. Cold Spring Harbor Laboratory, Cold Spring Harbor, N. Y. 969–986.
43. WRIGLEY, N. G. 1968. The lattice spacing of crystalline catalase as an internal standard of length in electron microscopy. *J. Ultrastruct. Res.* **24**:454–464.